sustainability

MDPI

Article

Spatial and Temporal Variability of Precipitation Complexity in Northeast Brazil

Antonio Samuel Alves da Silva [1,*], Ikaro Daniel de Carvalho Barreto [1,*], Moacyr Cunha-Filho [2], Rômulo Simões Cezar Menezes [2], Borko Stosic [1] and Tatijana Stosic [1]

1 Departamento de Estatística e Informática, Universidade Federal Rural de Pernambuco, Av. Manoel Medeiros S/N, Dois Irmãos, Recife 52171-900, PE, Brazil
2 Departamento de Energia Nuclear, Universidade Federal de Pernambuco, Moraes Rego 1235, Cidade Universitária, Recife 50670-901, PE, Brazil
* Correspondence: antonio.sasilva@ufrpe.br (A.S.A.d.S.); daniel.carvalho.ib@gmail.com (I.D.d.C.B.)

Abstract: In this work, we analyze the regularity of monthly rainfall temporal series during the period 1953 to 2012, recorded at 133 gauging stations in the state of Pernambuco, northeastern Brazil. We use sample entropy method (SampEn), which is suitable for short and noisy data and recently attracted the attention of hydrologists as promising for rainfall studies. By comparing the SampEn values of the analyzed series, we find that for both the original and deseasonalized series entropy increases (regularity decreases) in the west–east direction from the inland *Sertão* region towards the coastal *Zona da Mata*. SampEn values for the semiarid *Sertão* region are significantly different from the humid coastal *Zona da Mata* and subhumid transition *Agreste* regions. By comparing two 30 year subperiods (1953–1982 and 1983–2012), we found that in the second period, the rainfall amount decreases in *Sertão* and *Agreste*, and increases in Zona de Mata, and that the *Agreste* and *Zona da Mata* regions become more similar in respect to the regularity of rainfall dynamics. In the second subperiod, the rainfall regime changes the most in *Zona da Mata* (both original and anomalies series show a significant difference in SampEn values). By analyzing time dependent SampEn, we identified several periods of increasing entropy, which are related to specific climatic phenomena such as subsequent El Niño and La Niña episodes. This work represents a contribution to establishing the use of information theory-based methods in climatological studies.

Keywords: rainfall; sample entropy; time series regularity

check for updates

Citation: Silva, A.S.A.d.; Barreto, I.D.d.C.; Cunha-Filho, M.; Menezes, R.S.C.; Stosic, B.; Stosic, T. Spatial and Temporal Variability of Precipitation Complexity in Northeast Brazil. *Sustainability* **2022**, *14*, 13467. https://doi.org/10.3390/su142013467

Academic Editors: Dongwei Liu, Entao Yu and Qian Xia

Received: 13 September 2022
Accepted: 12 October 2022
Published: 19 October 2022

1. Introduction

The changes in rainfall patterns in the tropics can cause extreme conditions such as droughts and floods that severely affect human life, food and water security, infrastructure, biodiversity, and ecosystems health [1–4]. The semiarid region of northeastern Brazil (NEB) (which includes the larger area of the states of Piauí, Ceará, Rio Grande do Norte, Paraíba, Pernambuco, Alagoas, Sergipe, and Bahia), with an area of nearly 1,000,000 km^2 (12% of Brazilian territory) and more than 27 million inhabitants, is one of the world's most densely populous dryland regions. The population relies strongly on agriculture, livestock, and forestry production for subsistence and, therefore, is extremely vulnerable to climate changes [5]. Inter-annual climate variability in NEB is rather pronounced, and both global and regional climate change models suggest that the region will be affected by further rain deficits and increased aridity in the second half of the 21st century [6]. The rainfall pattern over NEB is highly seasonal, due to the influence of the Atlantic intertropical convergence zone (ITCZ) and South American monsoon system (SAMS). In most of NEB, the rainy season is from February to April, with severe droughts and floods that are related to the El Niño—Southern Oscillation (ENSO) in the equatorial Indo–Pacific Ocean, and the meridional sea surface temperature gradient (MGRAD) over the tropical Atlantic. Decreased rainfall is observed during positive El Niño phase of ENSO and negative phase of MGRAD, while during the negative La Niña phase of ENSO and positive phase of MGRAD, the precipitation rate is above the average [7]. In ENSO years in which Atlantic Sea surface temperature (SST) anomalies are such that they amplify the direct impact of ENSO, NEB can be affected by prolonged drought periods [8], which can cause serious economic, social, and environmental consequences [5].

Rainfall is one of the most important variables used in climate change studies [9,10]. Long-term variability of temperature and precipitation is extensively studied at both global and local scale [11,12], including Brazilian data [13–15]. On the other hand, most of the literature on spatial and temporal distribution of rainfall in NEB focuses on the interior dry region [16–18], while less is known about rainfall patterns of the eastern and southern parts of the region [19–21].

Over the last decades, novel concepts and methods from complex system science have been increasingly used to assess the degree of nonlinearity and overall complexity of rainfall dynamics. Such methods include chaos theory [22,23], fractal and multifractal analysis [24–26], information measures [27,28], and complex networks [29–31]. While fractal, multifractal, and complex network methods were extensively used to analyze the temporal and spatial variability of rainfall, far less is known about the properties of rainfall dynamics that can be detected by methods based on information theory. Various entropy measures were used to describe irregularity and rate of information flow in hydrological data, and proved useful to access changes caused by natural and human factors [32–34]. Sample entropy (SampEn) measures the time series regularity by counting similar patterns within a certain tolerance level and calculating the conditional probability that two similar sequences of m points remain similar at the next point m + 1, where self-matches are not included [35]. Originally developed for physiological applications, SampEn does not require any previous knowledge about the source generating the dataset, and is robust to noise and time series length, which facilitates its applicability in a wide variety of research fields [36]. Recently, the SampEn method was successfully applied in rainfall studies providing new information about the complexity of rainfall dynamics and its spatiotemporal variability [37–40].

In this work, we contribute to a better understanding of the spatiotemporal rainfall distribution in the Brazilian northeast, specifically the state of Pernambuco, a large part of which (about 70%) is in the semiarid region known as “Drought Polygon” (*Polígono das Secas*), being extremely vulnerable to rainfall seasonal and interannual variability. We use the SampEn method to analyze monthly time series recorded at 133 pluviometric stations during the period 1953 to 2012, and analyze the spatial distribution of entropy values to compare rainfall regimes among different climate zones. We also compare SampEn values for two 30 year subperiods (1953–1982 and 1983–2912), and we perform a time-dependent analysis (in sliding windows of 10 years) that provides more detailed information about the rainfall temporal regularity and relation to large scale climatic phenomena.

2. Materials and Methods

2.1. Study Area and Dataset

The state of Pernambuco is located in the eastern part of the northeast of Brazil, between the parallels 7°15′45′′ S and 9°28′18′′ S and meridians 34°48′33′′ W and 41°19′54′′ W. It is bordered by the states of Alagoas and Bahia (south), Piaui (west), Paraiba and Ceará (north), and the Atlantic Ocean to the east. The humid Atlantic Forest zone (*Zona da Mata*) stretches about 70 km from the sea to the Borborema mountain chain, while the semiarid region (*Sertão*) is located to the west of the Borborema chain, and the sub-humid transition zone (*Agreste*) is located between the *Zona da Mata* and *Sertão*. In the coastal area, the climate is humid tropical with the strong east to west rainfall gradient (from 1500 to 700 mm), with the rainy season between May and July and the intense dry season between September and December. In the *Sertão* region, the climate is semiarid with around 500 mm or less of total annual rainfall. The rainy season is short, concentrated from February to April, and the dry period lasts nine months [41]. Due to climate variability, Pernambuco experiences both recurrent droughts in *Sertão*, and floods in the coastal region.

The data used in this work are historical series of monthly rainfall for the state of Pernambuco, Brazil, recorded at 133 meteorological stations during the period 1953 to 2012. The data are provided by the Meteorological Laboratory of the Institute of Technology of Pernambuco (Laboratório de Meteorologia do Instituto de Tecnologia de Pernambuco—LAMEP/ITEP) [42]. The spatial distribution of the ITEP weather stations is shown in Figure 1.

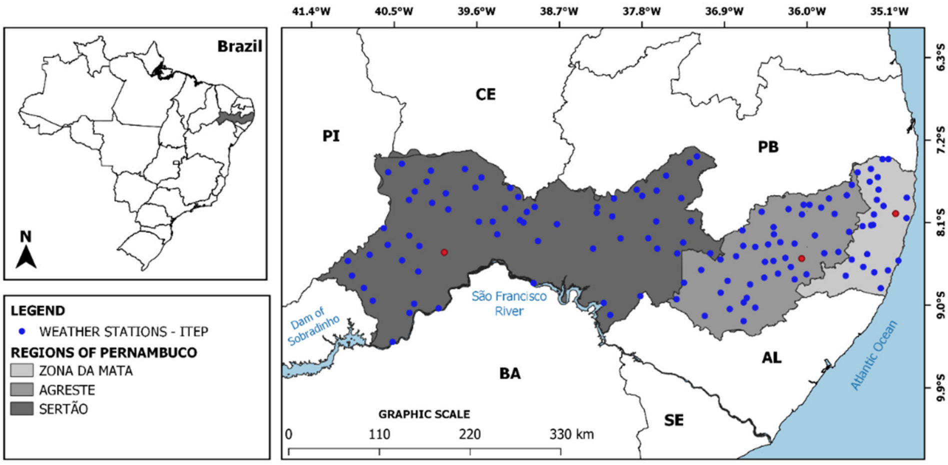

Figure 1. Geographical location of the state of Pernambuco, Brazil, and the spatial distribution of the ITEP weather stations. Red circles show the locations of three representative stations in Zona de Mata (São Lourenço da Mata, lat = −8.00, lon = −35.04) *Agreste* (Altinho, lat = −8.49, lon = −36.06), and *Sertão* (Santa Maria da Boa Vista, lat = −8.42, lon = −39.95) region.

2.2. Sample Entropy (SampEn)

Sample entropy ($SampEn$) was introduced by Richman and Moorman [35] as a measure of the rate of generation of new information in temporal series. For time series of length N $SampEn(m, r, N)$ is defined as the negative natural logarithm of the conditional probability that two sequences that are similar for m points (within tolerance level r) remain similar at the next point, where probability calculation does not include self-matches. Thus, the time series that contains more frequent and more similar sequences is more regular and displays lower values of $SampEn$. Sample entropy method is used in data analysis in physiology [43,44], geophysics [45], hydrology [28,32,37,38], engineering [46], and finances [47,48]. The algorithm that calculates sample entropy consists of the following steps [35]:

(i) For a time series of length N, $u(i),\ i = 1, \ldots, N$, we form $N - m + 1$ m—dimensional template vectors $x_m(i) = \{u(i + k) : k = 0, \ldots, m - 1\},\ i = 1, \ldots, N - m + 1$;

(ii) The distance between vectors $x_m(i)$ and $x_m(j)$ is defined as a maximum difference of their corresponding scalar components:

$$d[x_m(i),\ x_m(j)] = \max\{|u(i + k) - u(j + k)| : k = 0, \ldots, m - 1\}$$

(iii) We count the number B_i of vectors $x_m(j)$, such that $d[x_m(i),\ x_m(j)] \leq r\sigma$, where r is a tolerance level of accepting matches, σ is the standard deviation of $u(i),\ i = 1, \ldots, N$), and $j \neq i$ to exclude self-matches. If the original data are normalized by dividing by σ, the similarity criterion becomes $d[x_m(i),\ x_m(j)] \leq r$, as implemented in the current work;

(iv) We define

$$B_i^m(r) = \frac{B_i}{N - m + 1} \text{ and } B^m(r) = \frac{\sum_{i=1}^{N-m} B_i^m(r)}{N - m}$$

where $B_i^m(r)$ is the probability that two vectors will match for m points;

(v) We repeat steps (i)–(iv) for vectors of length $m+1$ and define

$$A_i^m(r) = \frac{A_i}{N-m+1} \text{ and } A^m(r) = \frac{\sum_{i=1}^{N-m} A_i^m(r)}{N-m}$$

where A_i is a number of vectors $x_{m+1}(j)$ that are similar (within r) to $x_{m+1}(i)$ and $A^m(r)$ is the probability that two vectors will match for $m+1$ points;

(vi) Sample entropy (SampEn) is defined as

$$SampEn(m,r,N) = \lim_{N\to\infty}\left[-ln\frac{A^m(r)}{B^m(r)}\right]$$

that is estimated by the statistics

$$SampEn(m,r,N) = -ln\frac{A^m(r)}{B^m(r)}$$

2.3. Time-Dependent SampEn

For a time series $x_1,\ldots,\ x_N$, the sliding window is defined as $X_t = x_t,\ x_{t+1},\ \ldots,\ x_{t+w-1}$, where w $\leq$ N is the window size and $t = 1, 2, \ldots N-w$. Values of the time series in each window X_t are used to calculate the SampEn (m,r,w) at a given time t, which provides the quantification of irregularity in the series as a function of time.

3. Results and Discussions

We analyze the original and the deseasonalized (anomalies) rainfall series for all 133 pluviometric stations. The rainfall anomalies are calculated as:

$$X(t) = \frac{x(t) - \mu_t}{\sigma_t}$$

where μ_t is the mean monthly rainfall calculated for each calendar month by averaging over all the years in the record, and σ_t is the standard deviation of $x(t)$, also calculated for each calendar month. The original and the anomalies series for three stations from *Zona da Mata*, *Agreste,* and *Sertão* are shown in Figure 2. The parameters used for SampEn calculation are m = 2 and r = 0.2, as recommended in [35], and is used in most applications.

3.1. Spatio-Temporal Exploratory Data Analysis

The spatial distribution of mean annual accumulated rainfall over the entire state is shown in Figure 3, where it is seen that the amount of annual rainfall decreases in an east–west direction: more rainfall in the coastal *Zona da Mata* region, much less rain in the inland semiarid *Sertão* region, and an intermediate rainfall amount in the transition *Agreste* region. A similar pattern is observed for the rainfall original series for the three representative stations in Figure 2a. Anomalies series (Figure 2b) show different behavior, with higher anomalies values in *Sertão* than in *Zona da Mata*, reflecting the difference in rainfall regime in these two regions: in *Sertão* dry and wet periods are well-defined and more pronounced than in *Zona da Mata,* for which rainfall is more uniformly distributed throughout the analyzed period.

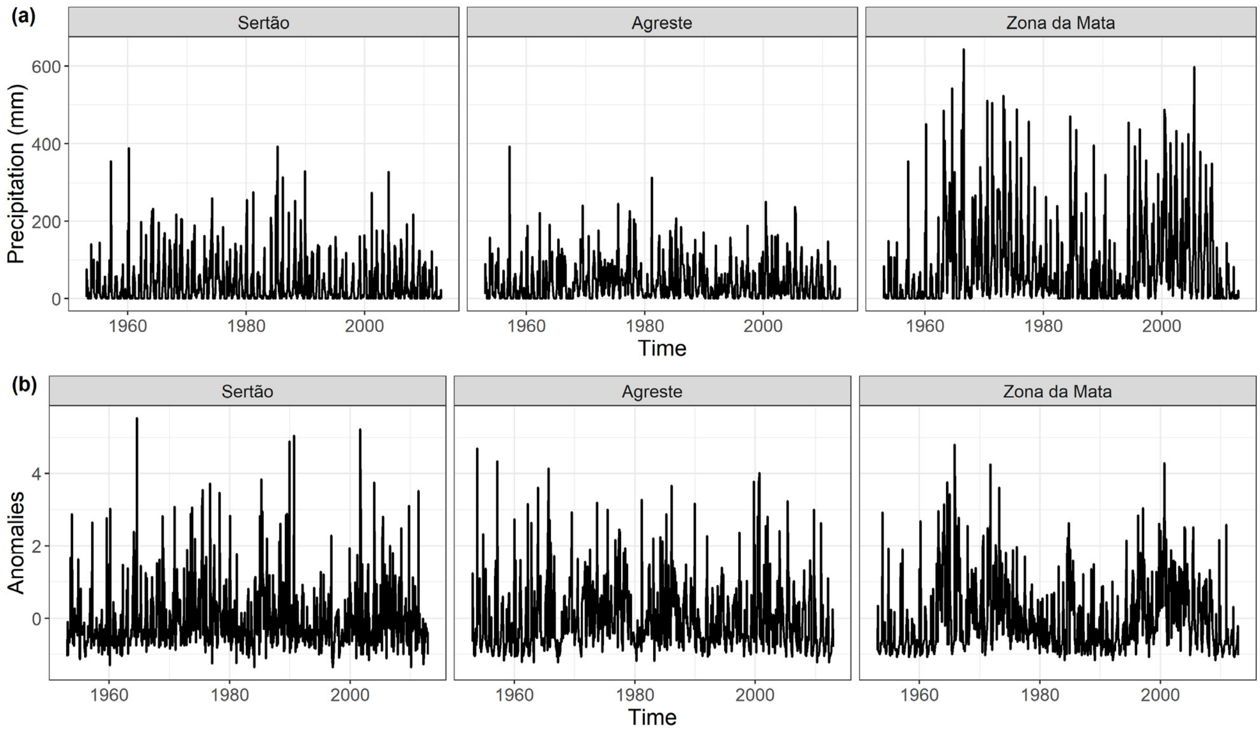

Figure 2. Original (**a**) and anomalies (**b**) monthly rainfall time series, recorded in three representative stations.

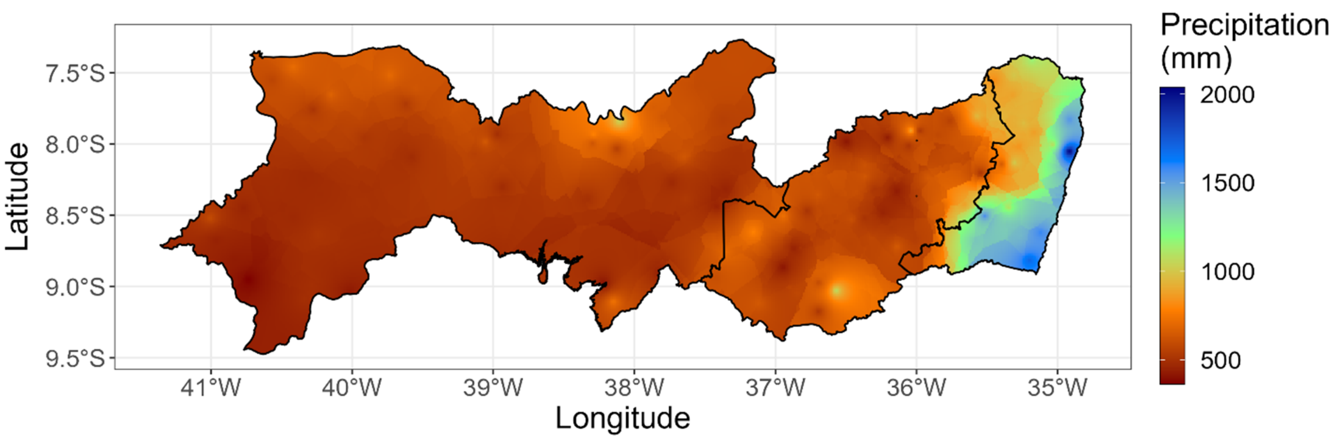

Figure 3. Mean yearly accumulated rainfall data interpolated over the state of Pernambuco.

3.2. SampEn (1953–2012)

The spatial distribution of the SampEn values for the original series and anomalies across the state of Pernambuco, obtained by interpolation of SampEn results for all 133 stations, are shown in Figure 4, where we observe the following pattern: (i) due to strong seasonality, the original series are more regular and show lower entropy values than anomalies series where the seasonality is removed; (ii) for both, original series and anomalies entropy increases (regularity decreases) in the west–east direction from the inland *Sertão* region (with semiarid climate and well-defined wet and dry yearly period) towards the coastal *Zona da Mata* (with humid climate, and more irregularly distributed rain throughout a year).

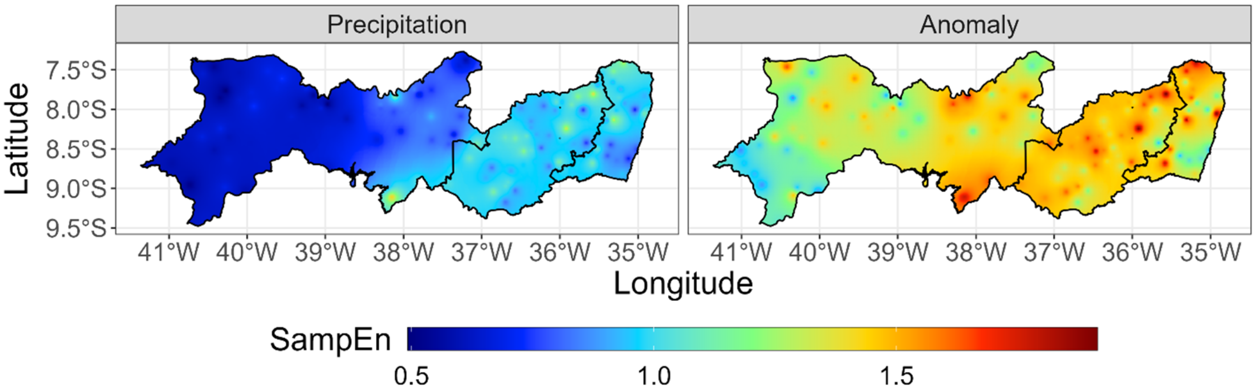

Figure 4. Spatial distribution of *SampEn* for original and anomalies series for period 1953–2012.

In order to assess the difference in entropy values between each of the regions, we construct boxplots of SampEn (Figure 5) and perform the Wilcoxon–Mann–Whitney test [49] at the 5% significance level. For original series, there is a significant difference between *Sertão* and *Agreste*, and between *Sertão* and *Zona da Mata*, while for anomalies series, a significant difference is found only between the *Sertão* and *Agreste* stations.

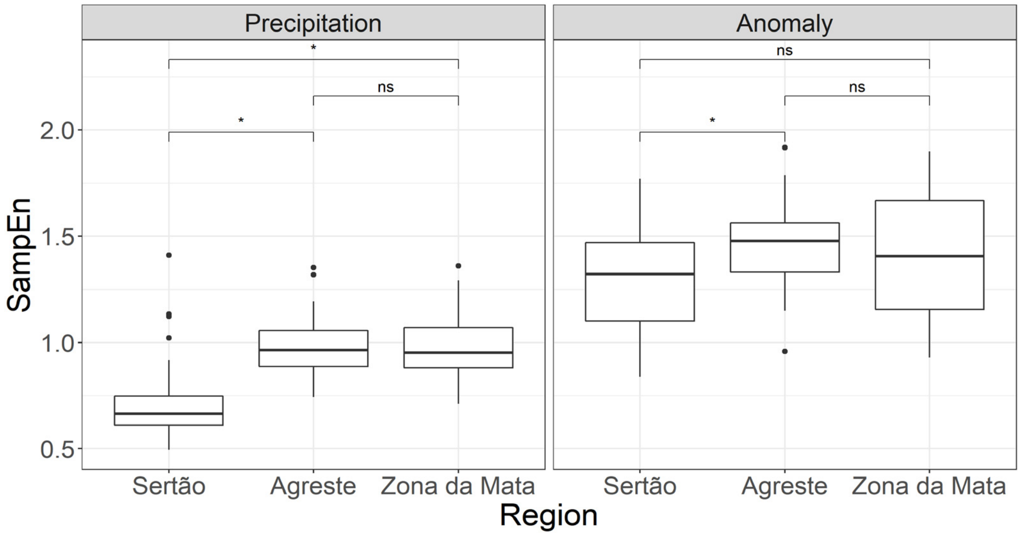

Figure 5. Boxplots for SampEn for original and anomalies series for the period 1953–2012. Symbol "*" indicates that there is a significant difference between the regions at the 5% significance level and "ns" means not significant.

3.3. SampEn: Comparing Subperiods of 1953–1982 and 1983–2012

In order to investigate whether the rainfall regularity has changed over the analyzed period, we calculate the SampEn values of the original and anomalies series for two 30 year subperiods: 1953–1982 and 1983–2012. The mean yearly accumulated rainfall for these subperiods is shown in Figure 6, where it is observed that in the second period, rainfall amount decreases in *Sertão* and *Agreste*, and increases in Zona de Mata. This is the result of ongoing climate changes, and it is expected that these changes in tropical rainfall will continue through the effects on both atmospheric moisture and circulation, in such a way as to reduce precipitation and increase evaporation in already dry regions, so that they become even dryer, and causing the opposite effects in already wet regions, that become wetter [1].

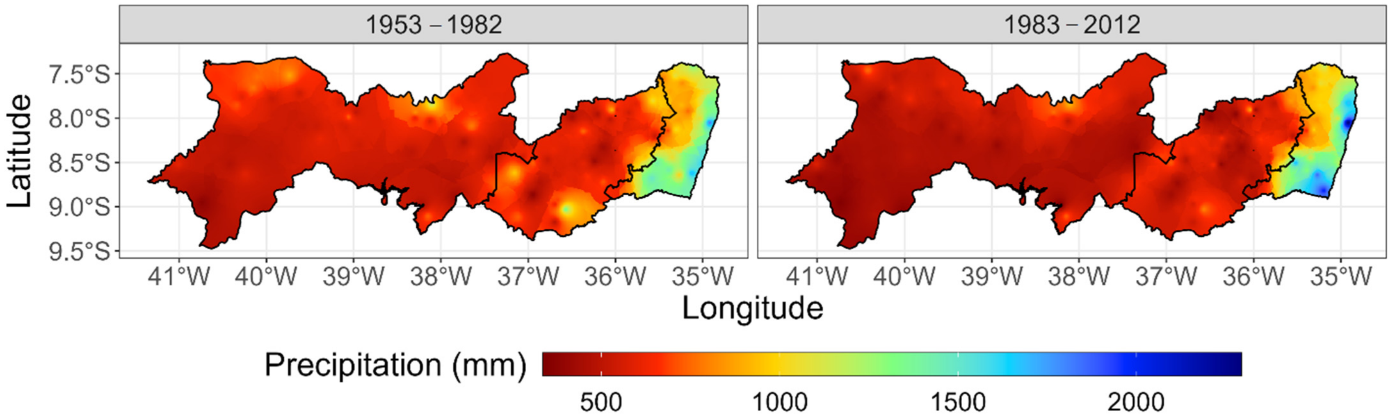

Figure 6. Mean yearly accumulated rainfall data for two subperiods (1953–1982 and 1983–2012) interpolated over the state of Pernambuco.

The spatial distribution of SampEn values for two subperiods (interpolated from the results of all 133 stations) is shown in Figure 7. By looking at the color code, we can observe that for original series, the entropy of rainfall series in *Zona da Mata* increases in the second period, indicating more irregular rainfall dynamics in the coastal region. For anomalies series, an increase in entropy is observed for *Zona da Mata* and *Agreste*, while in the eastern part of *Sertão*, we observe a decrease in entropy. This finding is confirmed in Figure 8, which shows the difference in *SampEn* for original and anomalies series for the two subperiods.

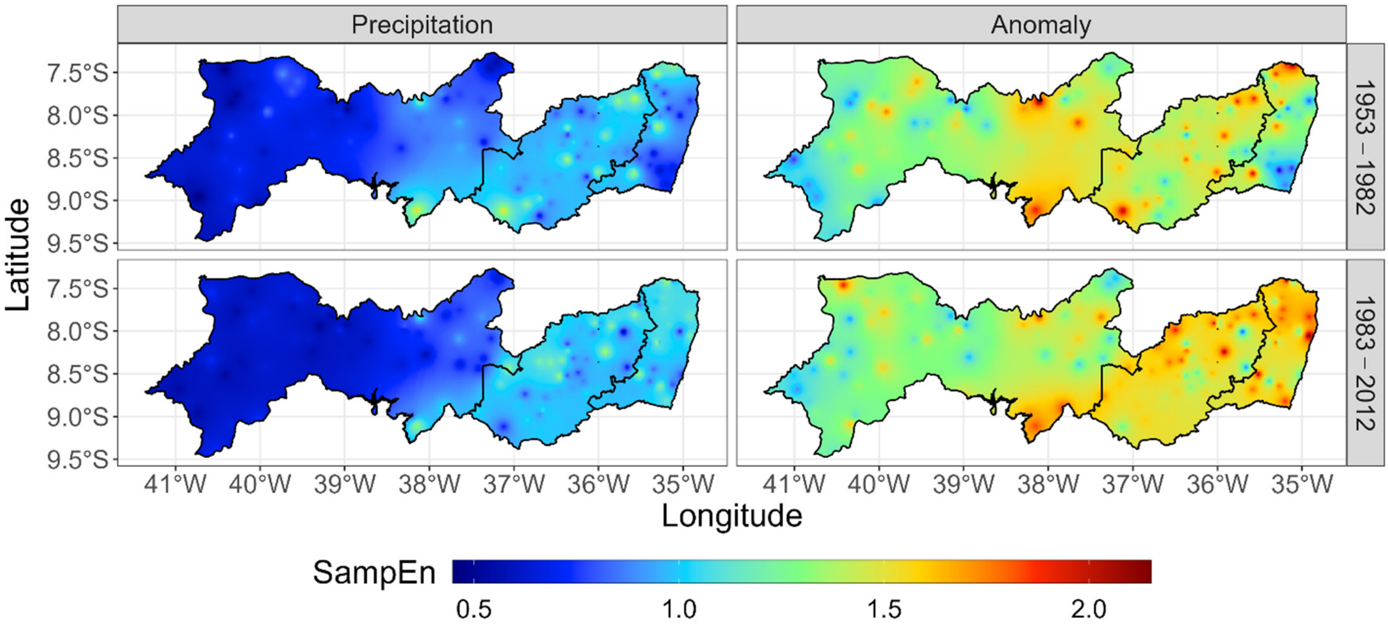

Figure 7. Spatial distribution of *SampEn* for original and anomalies series for two subperiods: 1953–1982 and 1983–2012.

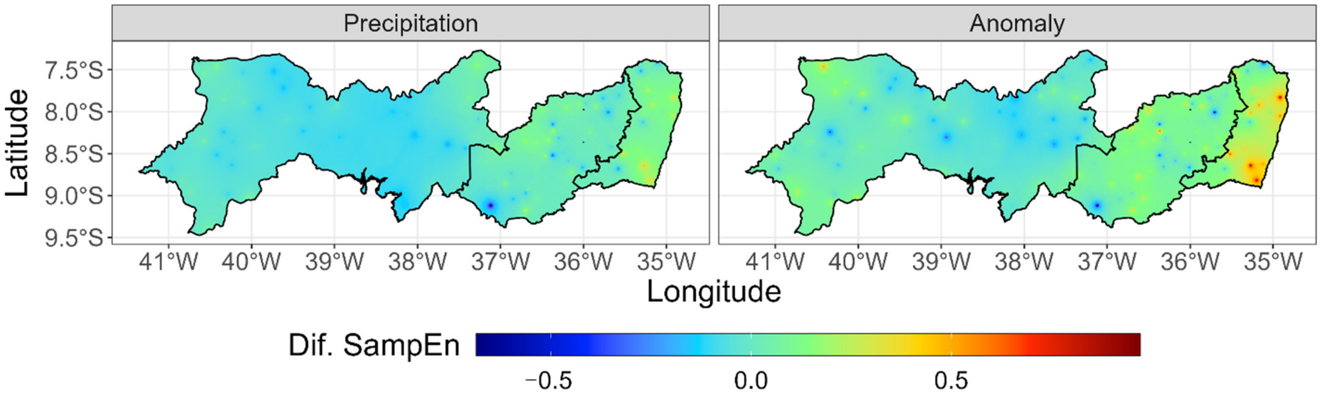

Figure 8. Spatial distribution of the difference of *SampEn* for original and anomalies series for two subperiods: 1953–1982 and 1983–2012.

In order to assess the difference in entropy values between the regions with respect to the two subperiods, we construct boxplots of SampEn between each of the regions for the first and the second subperiod (Figure 9), and for each region considering two subperiods (Figure 10), and we perform the Wilcoxon–Mann–Whitney test [49] at the 5% significance level. It is seen from Figure 9 that the test results for the original series indicate that there is a significant difference between all regions in the first subperiod, while in the second subperiod, the difference does not remain for *Agreste* and *Zona da Mata*, confirming what is observed in Figure 7 (by analyzing color code). For the anomalies series, the same observation stands for the second subperiod, while for the first subperiod no significant difference is found among regions. These results indicate that in the second subperiod, the *Agreste* and *Zona da Mata* regions become more similar with respect to the regularity of rainfall dynamics. A comparison of SampEn values for each region for the two subperiods (Figure 10) indicates that the rainfall regime changes the most in *Zona da Mata* (both original and anomalies series show significant difference in SampEn values), while in *Sertão* a significant difference between two periods is found for the original series, and in *Agreste* for the anomalies series.

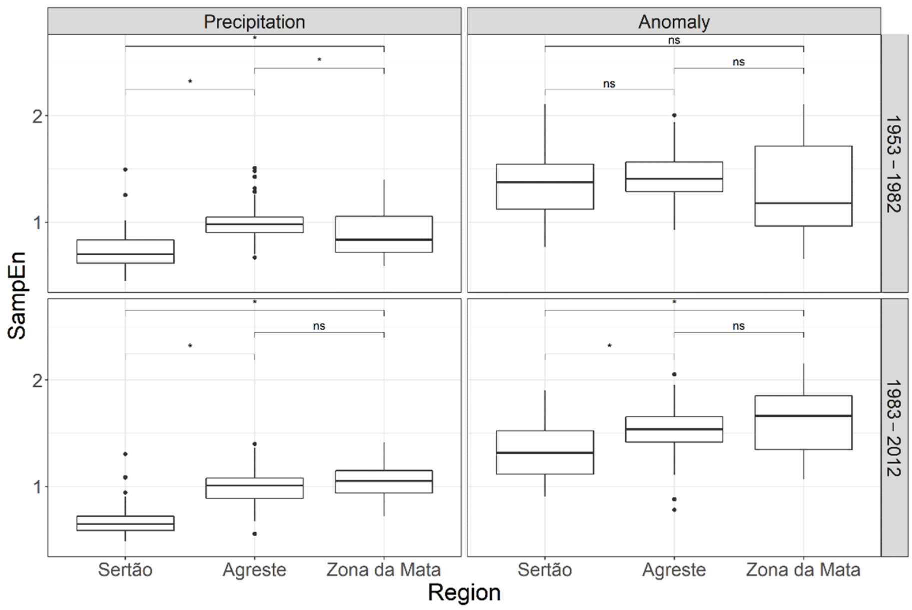

Figure 9. Boxplots for SampEn for original and anomalies series for two subperiods:1953–1982 and 1983–2012. Symbol "*" indicates that there is a significant difference between the regions at the 5% significance level and "ns" means not significant.

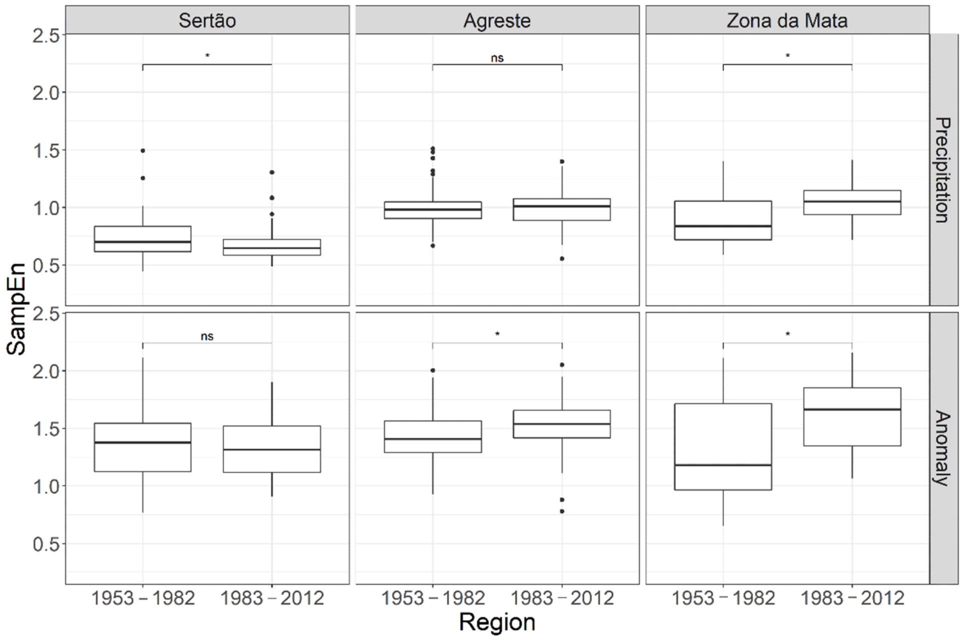

Figure 10. Boxplots for SampEn for original and anomalies series for *Sertão*, *Agreste*, and Zona de Mata (comparing two subperiods: 1953–1982 and 1983–2012.) Symbol "*" indicates that there is a significant difference between the regions at the 5% significance level and "ns" means not significant.

In the next step of our analysis, we calculate SampEn values for sliding windows of 120 months, with a sliding step of 1 month, using m = 2 and r = 0.2. The time evolution of these values for the original series and anomalies for three representative stations is shown by the blue lines in Figures 11 and 12, respectively.

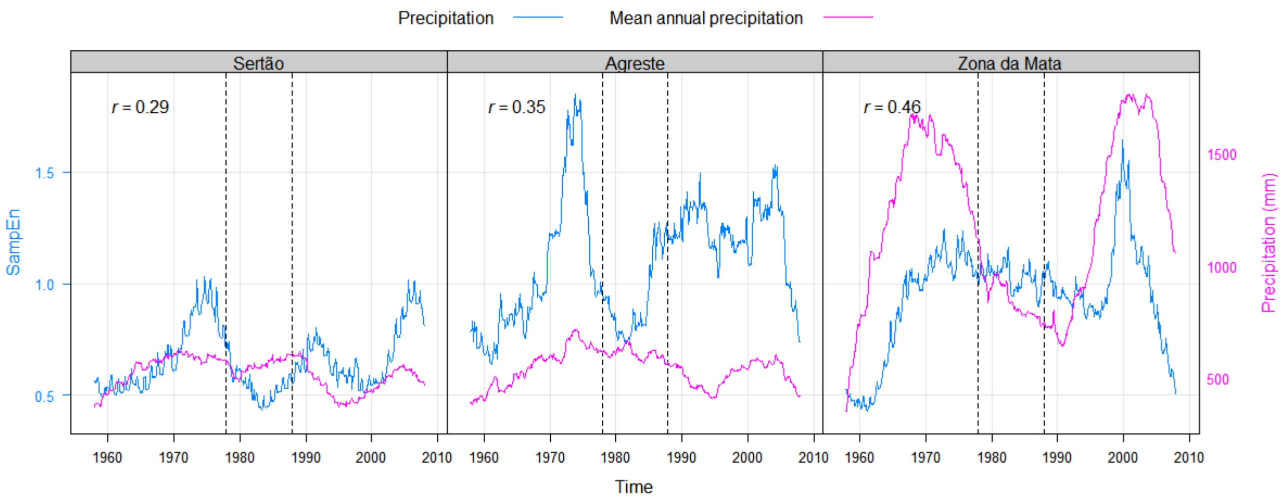

Figure 11. Temporal evolution of *SampEn* for original rainfall series for three representative stations in *Zona da Mata*, *Agreste*, and *Sertão*. Significant correlation, (r), $p < 0.05$, between *SampEn* (blue line) and mean annual anomaly (magenta line). The windows are presented with their midpoint. The vertical lines indicate midpoint of the end of the first time period (12/1977) and the midpoint of the beginning of the second time period (12/1987).

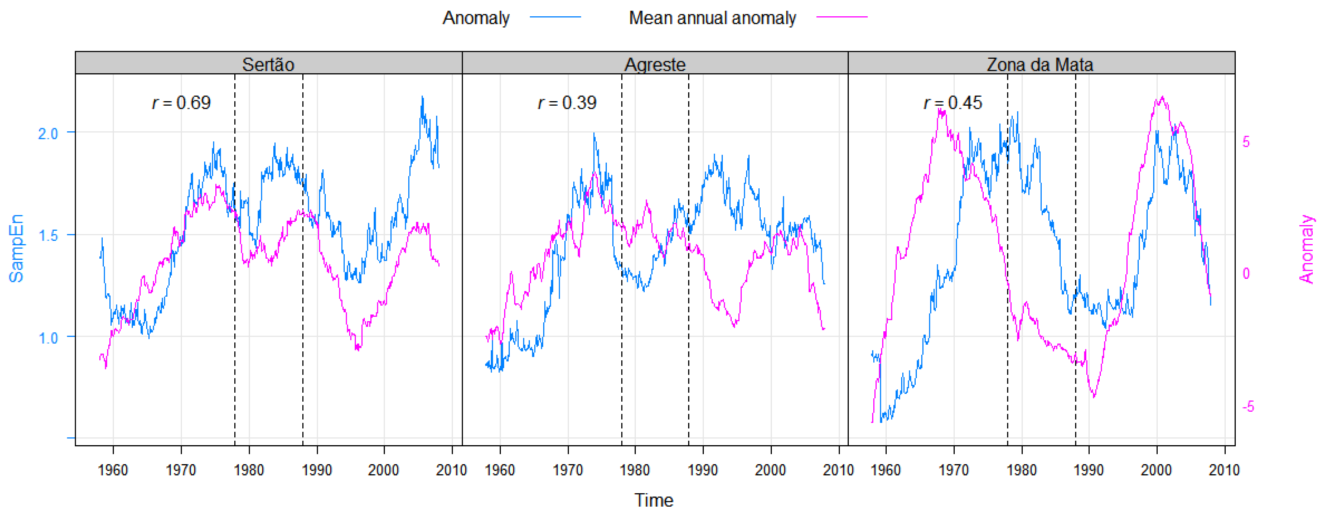

Figure 12. Temporal evolution of *SampEn* (blue line) for anomaly series for three representative stations in *Zona da Mata*, *Agreste*, and *Sertão* regions. Significant correlation, (r), $p < 0.05$, between *SampEn* (blue line) and mean annual anomaly (magenta line). The windows are presented with their midpoint. The vertical lines indicate midpoint of the end of the first time period (12/1977) and the midpoint of the beginning of second time period (12/1987).

The windows are represented by their midpoints, and the vertical dotted lines indicate the midpoint of the last window in the first period (1963–1987), and the midpoint of the first window of the second period (1988–2012). We observe that due to rainfall seasonality, the original series show lower entropy values (higher regularity) than the anomalies series in which seasonality is removed. We also identify several periods of increasing entropy, which are related to specific climatic phenomena: strong or moderate El Niño episodes succeeded by strong or moderate La Niña episodes, and vice versa [50]. 51We observe those periods in 1968–1977 (El Niño in 1969–1970 and in 1972–1973 was succeeded by La Niña in 1970–1971 and in 1973–1974; La Niña in 1975–1976 was succeeded by El Niño in 1976–1977), 1997–1999 (El Niño in 1997–1998 was succeeded by La Niña 1998–1999), and 2006–2008 (El Niño in 2006–2007 was succeeded by La Niña in 2007–2008). For the original series (Figure 11), we observe the periods of increasing entropy (increasing irregularity) in 1968–1977 for all the three regions, 1997–1999 for *Agreste* and Zona de Mata, and 2006–2008 for *Sertão* and *Agreste*. For anomalies series (Figure 12), we observed the same tendency in 1968–1977 for all three regions, 1997–1999 for *Sertão* and *Zona da Mata*, and 2006–2008 only for *Agreste*. For *Sertão* and *Agreste*, we identify one more period of increasing entropy: 1986–1989, when an El Niño episode was succeeded by a La Niña episode. In general, a reduction in precipitation in NEB is observed during El Niño episodes, while the increased precipitation in this same region is related to La Niña episodes [51]. Therefore, based on these observations, it may be expected that the successive episodes of increased and decreased rainfall result in a higher degree of irregularity in rainfall dynamics, and, thus, higher entropy values. This effect is most pronounced in the *Agreste* region (climate transition zone), for which the increase in entropy is observed for all periods, for both the original series and the anomalies. Along SampEn evolution, we also show the evolution of mean annual rainfall (Figure 11, magenta line) and mean annual anomaly (Figure 12, magenta line), together with the corresponding correlation coefficient, where we observe the following pattern: (i) for all cases the correlation is positive; (ii) for *Agreste* and *Zona da Mata*, correlation coefficients show similar values for both original and anomalies series, while for *Sertão*, correlation between SampEn and anomalies is stronger than between SampEn and original series; (iii) comparing correlations between SampEn and anomalies, we observe the strongest correlation for the *Sertão* region, while *Zona da Mata* shows the strongest correlation between SampEn and the original rainfall series.

We next implement the sliding window technique on all 133 stations, and for each station, we calculate mean SampEn values for all windows for the two subperiods and perform the Wilcoxon test. We, thus, classify the change between periods according to different levels of probability as proposed in Ref [52]. The results for two subperiods are shown in Figure 13 (original series) and Figure 14 (anomalies). It is seen from Figure 13 that: (i) in the most of the *Sertão* region, the SampEn changes are negative (decrease in entropy and increase in regularity in the second subperiod), while in *Agreste* and *Zona da Mata* they are positive (increase in entropy and decrease in regularity in the second subperiod), however there are some "islands" of positive change in *Sertão* and negative change in *Zona da Mata*. For anomalies (Figure 14) in most of Pernambuco state, the SampEn values have positive change from the first to the second subperiod, with some "islands" of negative changes. This result is consistent with what is observed in Figure 8: decrease in entropy in *Sertão* and increase in *Agreste* and *Zona da Mata* for the original series, and the increase in entropy for all regions for anomalies series.

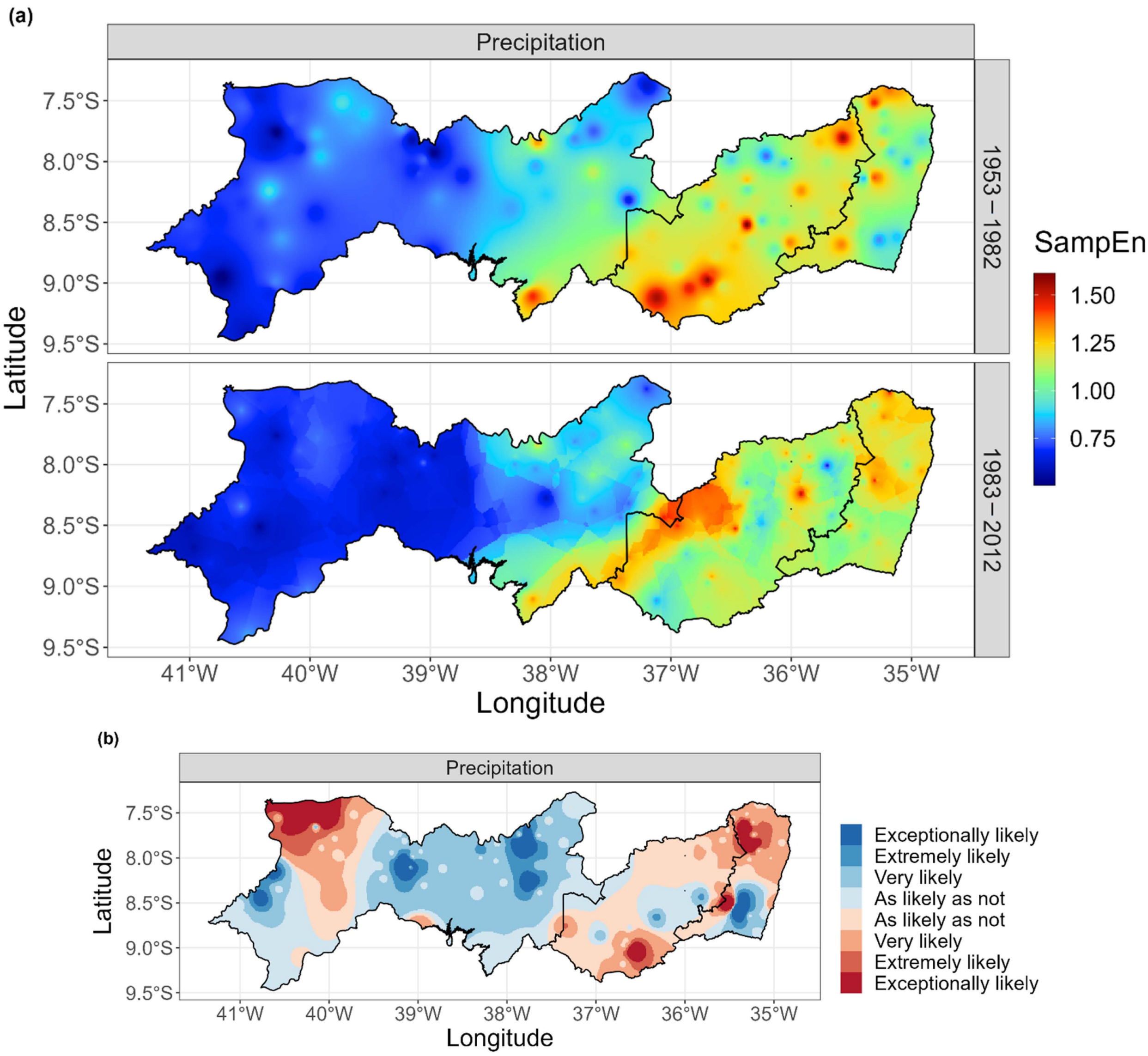

Figure 13. (**a**) Spatial distribution of mean SampEn values for original series (calculated from sliding windows) for first period (1953–1982) and second period (1983–2012); (**b**) the result of Wilcoxon test for each station. Changes between periods are classified according to different levels of probability: exceptionally likely ($p < 0.01$); extremely likely ($p < 0.05$); very likely ($p < 0.10$); as likely as not ($p > 0.10$). Blue color indicates negative change, red color stands for positive change.

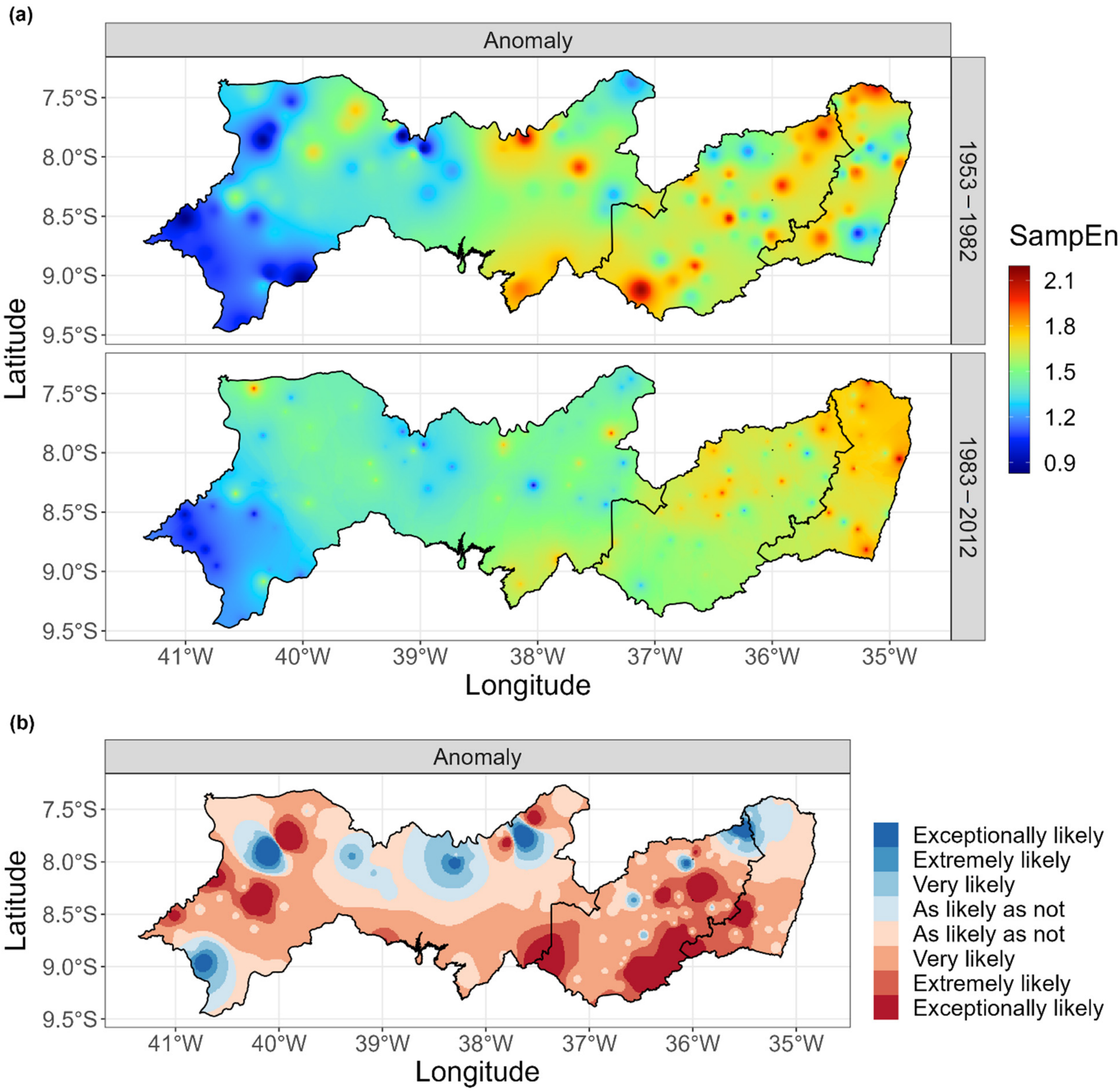

Figure 14. (**a**) Spatial distribution of mean SampEn values for anomalies series (calculated from sliding windows) for first period (1953–1982) and second period (1983–2012); (**b**) the result of Wilcoxon test for each station. Changes between periods are classified according to different levels of probability: exceptionally likely ($p < 0.01$); extremely likely ($p < 0.05$); very likely ($p < 0.10$); as likely as not ($p > 0.10$). Blue color indicates negative change, red color stands for positive change.

Finally, for each station we calculate the correlation coefficient between the temporal series of entropy and mean rainfall, and between entropy and mean rainfall anomaly, calculated in each sliding window (as shown in Figures 11 and 12 for the three representative stations). Then we interpolate the results to obtain the spatial distribution of the correlation coefficient, shown in Figure 15, where it is seen that, overall, for both original series and anomalies, the correlation is positive, which may be expected as both the annual rainfall (Figure 3) and entropy (Figure 4) show similar tendency (decrease in east–west direction). However, the correlation is stronger in the coastal *Zona da Mata* region (where more annual rainfall amount is irregularly distributed throughout a year) than in the semiarid *Sertão* region with less rain but more regularly distributed among the well-defined wet and dry periods.

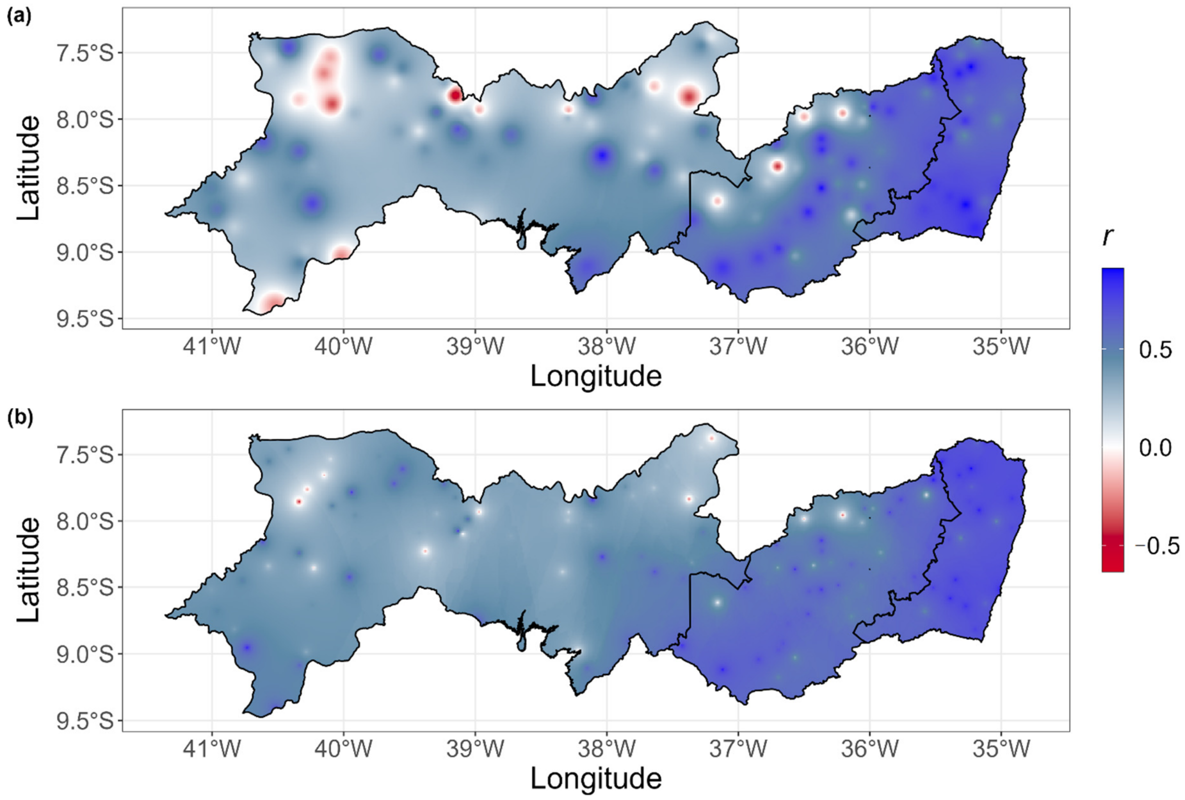

Figure 15. (**a**) Spatial distribution of correlation coefficient between SampEn and mean annual rainfall calculated in sliding windows; (**b**) spatial distribution of correlation coefficient between SampEn and mean annual anomalies calculated in sliding windows.

4. Conclusions

In this work, we analyzed rainfall temporal regularity for the state of Pernambuco, Brazil, in order to compare rainfall regimes in three regions: the coastal tropical humid Zona de Mata, the inland semiarid *Sertão* region, and the transitional sub-humid zone *Agreste*. We applied the sample entropy (SampEn) method to monthly rainfall series from 133 pluviometric stations during the period 1953 to 2012. For the entire recording period we found that: (i) due to strong seasonality, the original rainfall series show lower entropy (higher regularity) than the anomalies (deseasonalized) series; (ii) for both, original series and anomalies entropy increases (regularity decreases) in the west–east direction from the inland *Sertão* region towards coastal *Zona da Mata*; (iii) for the original series, there is a significant difference in entropy values between *Sertão* and *Agreste*, and between *Sertão* and *Zona da Mata*, while for the anomalies series, the significant difference is found only between *Sertão* and *Agreste*.

By comparing two 30 year subperiods (1953–1982 and 1983–2012), we found that: (i) in the second period, the rainfall amount decreases in *Sertão* and *Agreste*, and increases in Zona de Mata; (ii) for the original series, the entropy of rainfall series in *Zona da Mata* increases in the second period, indicating more irregular rainfall dynamics, while for the anomalies series, an increase in entropy (lower regularity) is observed for *Zona da Mata* and *Agreste*, and a decrease in entropy (higher regularity) in the eastern part of *Sertão*; (iii) in the second subperiod, the *Agreste* and Zona de Mata regions become more similar with respect to the regularity of rainfall dynamics (there is no significant difference in entropy values for both original and anomalies series); (iv) a comparison of SampEn values for each region for the two subperiods indicates that the rainfall regime changes the most in Zona de Mata (both original and anomalies series show significant difference).

The time evolution of rainfall regularity was analyzed by calculating SampEn values in 10 years sliding windows for all 133 monthly series, and applying statistical test for two

30 year subperiods. We found that from the first to the second subperiod for the original series, changes are negative in the *Sertão* region, and positive for *Agreste* and *Zona da Mata*, while for anomalies, in most of Pernambuco state the SampEn values show positive change.

By analyzing time-dependent SampEn for representative stations for each region, we identified several periods of increasing entropy that are related to specific climatic phenomena: strong or moderate El Niño episodes succeeded by strong or moderate La Niña episodes, and vice versa. Finally, by analyzing the correlation between the temporal series of entropy and mean rainfall calculated in 10 years sliding windows, we found that for both original series and anomalies, the correlation is positive and stronger in the coastal *Zona da Mata* region (where more annual rainfall amount is irregularly distributed throughout the year) than in the semiarid *Sertão* region with less rain but more regularly distributed among the well-defined wet and dry periods.

Our work provides a rather comprehensive analysis of rainfall temporal regularity in an area where climate and rainfall regime significantly vary (from the coastal subhumid and rainy Zona de Mata to the semiarid inland dry *Sertão* region). By applying SampEn method on long monthly records from many stations that are well-distributed across the study area, we are able to provide detailed spatiotemporal analysis of rainfall regime in Pernambuco state, to distinguish among different rainfall regimes, and to identify climatic phenomena such as consecutive El Niño and La Niña episodes. The results of our work together with other recent studies indicate that an information theory approach contributes to a deeper understanding of the mechanisms governing climate dynamics.

Author Contributions: Conceptualization, A.S.A.d.S., B.S. and T.S.; methodology, A.S.A.d.S., B.S. and T.S.; software, A.S.A.d.S.; validation, A.S.A.d.S., B.S., I.D.d.C.B. and T.S.; formal analysis, A.S.A.d.S., B.S., I.D.d.C.B. and T.S.; investigation, A.S.A.d.S., B.S. and T.S.; resources, A.S.A.d.S., B.S., R.S.C.M., M.C.-F. and T.S.; data curation, A.S.A.d.S., B.S. and R.S.C.M.; writing—original draft preparation, A.S.A.d.S., B.S., I.D.d.C.B. and T.S.; writing—review and editing, A.S.A.d.S., B.S., I.D.d.C.B., R.S.C.M. and T.S.; visualization, A.S.A.d.S.; supervision, A.S.A.d.S., B.S., R.S.C.M., M.C.-F. and T.S.; project administration, A.S.A.d.S., B.S., R.S.C.M., M.C.-F. and T.S.; funding acquisition, B.S., R.S.C.M. and M.C.-F. All authors have read and agreed to the published version of the manuscript.

Funding: CNPq 307445/2018-6, 304497/2019-3, 441305/2017-2; INCT-MCTI/CNPq/CAPES/FAPs 465764/2014-2; Facepe APQ-0296-5.01/17, APQ-0532-5.01/14.

Institutional Review Board Statement: Not applicable.

Informed Consent Statement: Not applicable.

Data Availability Statement: Not applicable.

Acknowledgments: The authors acknowledge support of Brazilian agencies CNPq, CAPES, and FACEPE through the following research grants: CNPq (441305/2017-2; 465764/2014-2; 304497/2019-3), CAPES (88887.136369/2017-00), and FACEPE (APQ-0296-5.01/17; APQ-0498-3.07/17 ONDACBC; APQ-0532-5.01/14).

Conflicts of Interest: The authors declare no conflict of interest.

References

1. Chadwick, R.; Good, P.; Martin, G.; Rowell, D.P. Large rainfall changes consistently projected over substantial areas of tropical land. *Nat. Clim. Chang.* **2016**, *6*, 177–181. [CrossRef]
2. Chretien, J.-P.; Anyamba, A.; Small, J.; Britch, S.; Sanchez, J.L.; Halbach, A.C.; Tucker, C.; Linthicum, K.J. Global Climate Anomalies and Potential Infectious Disease Risks: 2014–2015. *PLoS Curr.* **2015**, *7*. [CrossRef] [PubMed]
3. Stan, K.; Sanchez-Azofeifa, A. Tropical Dry Forest Diversity, Climatic Response, and Resilience in a Changing Climate. *Forests* **2019**, *10*, 443. [CrossRef]
4. D'Odorico, P.; Bhattachan, A. Hydrologic variability in dryland regions: Impacts on ecosystem dynamics and food security. *Philos. Trans. R. Soc. B Biol. Sci.* **2012**, *367*, 3145–3157. [CrossRef] [PubMed]
5. Marengo, J.A.; Torres, R.R.; Alves, L.M. Drought in Northeast Brazil—Past, present, and future. *Theor. Appl. Climatol.* **2017**, *129*, 1189–1200. [CrossRef]
6. Marengo, J.A.; Bernasconi, M. Regional differences in aridity/drought conditions over Northeast Brazil: Present state and future projections. *Clim. Change* **2015**, *129*, 103–115. [CrossRef]

7. Robertson, A.W.; Kirshner, S.; Smyth, P. Downscaling of Daily Rainfall Occurrence over Northeast Brazil Using a Hidden Markov Model. *J. Clim.* **2004**, *17*, 4407–4424. [CrossRef]
8. Giannini, A.; Saravanan, R.; Chang, P. The preconditioning role of Tropical Atlantic Variability in the development of the ENSO teleconnection: Implications for the prediction of Nordeste rainfall. *Clim. Dyn.* **2004**, *22*, 839–855. [CrossRef]
9. Dore, M.H.I. Climate change and changes in global precipitation patterns: What do we know? *Environ. Int.* **2005**, *31*, 1167–1181. [CrossRef]
10. Sun, Q.; Zhang, X.; Zwiers, F.; Westra, S.; Alexander, L. V A Global, Continental, and Regional Analysis of Changes in Extreme Precipitation. *J. Clim.* **2021**, *34*, 243–258. [CrossRef]
11. Alexander, L.V.; Zhang, X.; Peterson, T.C.; Caesar, J.; Gleason, B.; Klein Tank, A.M.G.; Haylock, M.; Collins, D.; Trewin, B.; Rahimzadeh, F.; et al. Global observed changes in daily climate extremes of temperature and precipitation. *J. Geophys. Res.* **2006**, *111*, D05109. [CrossRef]
12. Sun, W.; Mu, X.; Song, X.; Wu, D.; Cheng, A.; Qiu, B. Changes in extreme temperature and precipitation events in the Loess Plateau (China) during 1960–2013 under global warming. *Atmos. Res.* **2016**, *168*, 33–48. [CrossRef]
13. Regoto, P.; Dereczynski, C.; Chou, S.C.; Bazzanela, A.C. Observed changes in air temperature and precipitation extremes over Brazil. *Int. J. Climatol.* **2021**, *41*, 5125–5142. [CrossRef]
14. Marengo, J.A. Interdecadal variability and trends of rainfall across the Amazon basin. *Theor. Appl. Climatol.* **2004**, *78*, 79–96. [CrossRef]
15. Sansigolo, C.A.; Kayano, M.T. Trends of seasonal maximum and minimum temperatures and precipitation in Southern Brazil for the 1913–2006 period. *Theor. Appl. Climatol.* **2010**, *101*, 209–216. [CrossRef]
16. Hastenrath, S. Exploring the climate problems of Brazil's Nordeste: A review. *Clim. Change* **2012**, *112*, 243–251. [CrossRef]
17. Uvo, C.B.; Repelli, C.A.; Zebiak, S.E.; Kushnir, Y. The Relationships between Tropical Pacific and Atlantic SST and Northeast Brazil Monthly Precipitation. *J. Clim.* **1998**, *11*, 551–562. [CrossRef]
18. Oliveira, P.T.; Santos e Silva, C.M.; Lima, K.C. Climatology and trend analysis of extreme precipitation in subregions of Northeast Brazil. *Theor. Appl. Climatol.* **2017**, *130*, 77–90. [CrossRef]
19. Lyra, G.B.; Oliveira-Júnior, J.F.; Zeri, M. Cluster analysis applied to the spatial and temporal variability of monthly rainfall in Alagoas state, Northeast of Brazil. *Int. J. Climatol.* **2014**, *34*, 3546–3558. [CrossRef]
20. de Medeiros, E.S.; de Lima, R.R.; de Olinda, R.A.; de Santos, C.A.C. Modeling Spatiotemporal Rainfall Variability in Paraíba, Brazil. *Water* **2019**, *11*, 1843. [CrossRef]
21. da Silva, M.V.; Pandorfi, H.; Jardim, A.M.d.R.F.; Oliveira-Júnior, J.F.d.; Divincula, J.S.d.; Giongo, P.R.; Silva, T.G.F.d.; Almeida, G.L.P.d.; Moura, G.B.d.A.; Lopes, P.M.O. Spatial modeling of rainfall patterns and groundwater on the coast of northeastern Brazil. *Urban Clim.* **2021**, *38*, 100911. [CrossRef]
22. Fuwape, I.A.; Ogunjo, S.T.; Oluyamo, S.S.; Rabiu, A.B. Spatial variation of deterministic chaos in mean daily temperature and rainfall over Nigeria. *Theor. Appl. Climatol.* **2017**, *130*, 119–132. [CrossRef]
23. Sivakumar, B. Nonlinear dynamics and chaos in hydrologic systems: Latest developments and a look forward. *Stoch. Environ. Res. Risk Assess.* **2009**, *23*, 1027–1036. [CrossRef]
24. Sivakumar, B. Fractal analysis of rainfall observed in two different climatic regions. *Hydrol. Sci. J.* **2000**, *45*, 727–738. [CrossRef]
25. Kantelhardt, J.W.; Koscielny-Bunde, E.; Rybski, D.; Braun, P.; Bunde, A.; Havlin, S. Long-term persistence and multifractality of precipitation and river runoff records. *J. Geophys. Res. Atmos.* **2006**, *111*, 1–13. [CrossRef]
26. Adarsh, S.; Nourani, V.; Archana, D.S.; Dharan, D.S. Multifractal description of daily rainfall fields over India. *J. Hydrol.* **2020**, *586*, 124913. [CrossRef]
27. Mishra, A.K.; Özger, M.; Singh, V.P. An entropy-based investigation into the variability of precipitation. *J. Hydrol.* **2009**, *370*, 139–154. [CrossRef]
28. Xavier, S.F.A.; da Silva Jale, J.; Stosic, T.; dos Santos, C.A.C.; Singh, V.P. An application of sample entropy to precipitation in Paraíba State, Brazil. *Theor. Appl. Climatol.* **2019**, *136*, 429–440. [CrossRef]
29. Malik, N.; Bookhagen, B.; Marwan, N.; Kurths, J. Analysis of spatial and temporal extreme monsoonal rainfall over South Asia using complex networks. *Clim. Dyn.* **2012**, *39*, 971–987. [CrossRef]
30. Boers, N.; Goswami, B.; Rheinwalt, A.; Bookhagen, B.; Hoskins, B.; Kurths, J. Complex networks reveal global pattern of extreme-rainfall teleconnections. *Nature* **2019**, *566*, 373–377. [CrossRef]
31. Naufan, I.; Sivakumar, B.; Woldemeskel, F.M.; Raghavan, S.V.; Vu, M.T.; Liong, S.-Y. Spatial connections in regional climate model rainfall outputs at different temporal scales: Application of network theory. *J. Hydrol.* **2018**, *556*, 1232–1243. [CrossRef]
32. Zhang, Q.; Zhou, Y.; Singh, V.P.; Chen, X. The influence of dam and lakes on the Yangtze River streamflow: Long-range correlation and complexity analyses. *Hydrol. Process.* **2012**, *26*, 436–444. [CrossRef]
33. Stosic, T.; Telesca, L.; de Souza Ferreira, D.V.; Stosic, B. Investigating anthropically induced effects in streamflow dynamics by using permutation entropy and statistical complexity analysis: A case study. *J. Hydrol.* **2016**, *540*, 1136–1145. [CrossRef]
34. Ma, W.; Kang, Y.; Song, S. Analysis of Streamflow Complexity Based on Entropies in the Weihe River Basin, China. *Entropy* **2019**, *22*, 38. [CrossRef] [PubMed]
35. Richman, J.S.; Moorman, J.R. Physiological time-series analysis using approximate entropy and sample entropy. *Am. J. Physiol. Heart Circ. Physiol.* **2000**, *278*, H2039–H2049. [CrossRef] [PubMed]

36. Delgado-Bonal, A.; Marshak, A. Approximate Entropy and Sample Entropy: A Comprehensive Tutorial. *Entropy* **2019**, *21*, 541. [CrossRef]
37. Zhang, L.; Li, T.; Liu, D.; Fu, Q.; Li, M.; Faiz, M.A.; Ali, S.; Khan, M.I. Spatial variability and possible cause analysis of regional precipitation complexity based on optimized sample entropy. *Q. J. R. Meteorol. Soc.* **2020**, *146*, 3384–3398. [CrossRef]
38. Zhou, X.; Lei, W. Spatial patterns of sample entropy based on daily precipitation time series in China and their implications for land surface hydrological interactions. *Int. J. Climatol.* **2020**, *40*, 1669–1685. [CrossRef]
39. Du, L.; Li, X.; Yang, M.; Sivakumar, B.; Zhu, Y.; Pan, X.; Li, Z.; Sang, Y.-F. Assessment of spatiotemporal variability of precipitation using entropy indexes: A case study of Beijing, China. *Stoch. Environ. Res. Risk Assess.* **2022**, *36*, 939–953. [CrossRef]
40. Zhang, L.; Li, H.; Liu, D.; Fu, Q.; Li, M.; Faiz, M.A.; Khan, M.I.; Li, T. Identification and application of the most suitable entropy model for precipitation complexity measurement. *Atmos. Res.* **2019**, *221*, 88–97. [CrossRef]
41. Alvares, C.A.; Stape, J.L.; Sentelhas, P.C.; de Moraes Gonçalves, J.L.; Sparovek, G. Köppen's climate classification map for Brazil. *Meteorol. Z.* **2013**, *22*, 711–728. [CrossRef]
42. da Silva, A.S.A.; Stosic, B.; Menezes, R.S.C.; Singh, V.P. Comparison of Interpolation Methods for Spatial Distribution of Monthly Precipitation in the State of Pernambuco, Brazil. *J. Hydrol. Eng.* **2019**, *24*. [CrossRef]
43. Lake, D.E.; Richman, J.S.; Griffin, M.P.; Moorman, J.R. Sample entropy analysis of neonatal heart rate variability. *Am. J. Physiol. Integr. Comp. Physiol.* **2002**, *283*, R789–R797. [CrossRef] [PubMed]
44. Namazi, H. Complexity-based analysis of the correlation between stride interval variability and muscle reaction at different walking speeds. *Biomed. Signal Process. Control* **2021**, *69*, 102956. [CrossRef]
45. Balasis, G.; Daglis, I.A.; Papadimitriou, C.; Kalimeri, M.; Anastasiadis, A.; Eftaxias, K. Investigating dynamical complexity in the magnetosphere using various entropy measures. *J. Geophys. Res. Space Phys.* **2009**, *114*. [CrossRef]
46. Zhao, Z.H.; Yang, S. Sample entropy-based roller bearing fault diagnosis method. *J. Vib. Shock* **2012**, *31*, 136–140.
47. Efremidze, L.; Stanley, D.J.; Kownatzki, C. Entropy trading strategies reveal inefficiencies in Japanese stock market. *Int. Rev. Econ. Financ.* **2021**, *75*, 464–477. [CrossRef]
48. Batra, L.; Taneja, H.C. Evaluating volatile stock markets using information theoretic measures. *Phys. A Stat. Mech. Its Appl.* **2020**, *537*, 122711. [CrossRef]
49. Mann, H.B.; Whitney, D.R. On a Test of Whether one of Two Random Variables is Stochastically Larger than the Other. *Ann. Math. Stat.* **1947**, *18*, 50–60. [CrossRef]
50. CPTEC INPE. Available online: http://enos.cptec.inpe.br/ (accessed on 1 March 2022).
51. Kayano, M.T.; Andreoli, R.V. Relationships between rainfall anomalies over northeastern Brazil and the El Niño–Southern Oscillation. *J. Geophys. Res.* **2006**, *111*, D13101. [CrossRef]
52. de Luis, M.; González-Hidalgo, J.C.; Brunetti, M.; Longares, L.A. Precipitation concentration changes in Spain 1946–2005. *Nat. Hazards Earth Syst. Sci.* **2011**, *11*, 1259–1265. [CrossRef]